1521-009X/44/5/692–699$25.00
Drug Metabolism and Disposition

http://dx.doi.org/10.1124/dmd.115.067447
Drug Metab Dispos 44:692–699, May 2016

The Antimicrobial Agent Fusidic Acid Inhibits Organic Anion Transporting Polypeptide–Mediated Hepatic Clearance and May Potentiate Statin-Induced Myopathy

Heather Eng, Renato J. Scialis, Charles J. Rotter, Jian Lin, Sarah Lazzaro, Manthena V. Varma, Li Di, Bo Feng, Michael West, and Amit S. Kalgutkar

Pharmacokinetics, Pharmacodynamics, and Metabolism Department–New Chemical Entities, Pfizer Inc., Groton, Connecticut (H.E., R.J.S., C.J.R., J.L., S.L., M.V.V., L.D., B.F., M.W.); and Pharmacokinetics, Pharmacodynamics, and Metabolism Department–New Chemical Entities, Pfizer Inc., Cambridge MA (A.S.K.)

Received September 28, 2015; accepted February 12, 2016

ABSTRACT

Chronic treatment of methicillin-resistant *Staphylococcus aureus* strains with the bacteriostatic agent fusidic acid (FA) is frequently associated with myopathy including rhabdomyolysis upon coadministration with statins. Because adverse effects with statins are usually the result of drug–drug interactions, we evaluated the inhibitory effects of FA against human CYP3A4 and clinically relevant drug transporters such as organic anion transporting polypeptides OATP1B1 and OATP1B3, multidrug resistant protein 1, and breast cancer resistance protein, which are involved in the oral absorption and/or systemic clearance of statins including atorvastatin, rosuvastatin, and simvastatin. FA was a weak reversible (IC_{50} = 295 ± 1.0 μM) and time-dependent (K_I = 216 ± 41 μM and k_{inact} = 0.0179 ± 0.001 min^{-1}) inhibitor of CYP3A4-catalyzed midazolam-1′-hydroxylase activity in human liver microsomes. FA demonstrated inhibition of multidrug resistant protein 1–mediated digoxin transport with an IC_{50} value of 157 ± 1.0 μM and was devoid of breast cancer resistance protein inhibition (IC_{50} > 500 μM). In contrast, FA showed potent inhibition of OATP1B1- and OATP1B3-specific rosuvastatin transport with IC_{50} values of 1.59 μM and 2.47 μM, respectively. Furthermore, coadministration of oral rosuvastatin and FA to rats led to an approximately 19.3-fold and 24.6-fold increase in the rosuvastatin maximum plasma concentration and area under the plasma concentration–time curve, respectively, which could be potentially mediated through inhibitory effects of FA on rat Oatp1a4 (IC_{50} = 2.26 μM) and Oatp1b2 (IC_{50} = 4.38 μM) transporters, which are responsible for rosuvastatin uptake in rat liver. The potent inhibition of human OATP1B1/OATP1B3 by FA could attenuate hepatic uptake of statins, resulting in increased blood and tissue concentrations, potentially manifesting in musculoskeletal toxicity.

Introduction

Fusidic acid (FA; Fig. 1) is an orally active bacteriostatic antibiotic with wide clinical usage in Europe and Australasia for the treatment of methicillin-resistant *Staphylococcus aureus* and, more recently, multiresistant *Staphylococcus aureus* strains (Vanderhelst et al., 2013; Hall et al., 2015). Furthermore, in countries where FA is available, chronic oral therapy with FA is routinely used in the treatment of *Staphylococcus*-mediated prosthetic joint infections among the elderly population (Aboltins et al., 2007; Wang et al., 2012). The widespread clinical use of FA in suppressive antibiotic therapy is also associated with several cases of life-threatening rhabdomyolysis (with fatalities) upon coadministration with the 3-hydroxy-3-methylglutaryl CoA reductase inhibitors, atorvastatin and simvastatin (Wenisch et al., 2000; Yuen and McGarity, 2003; Burtenshaw et al., 2008; O'Mahony et al., 2008; Herring et al., 2009; Saeed and Azam, 2009; Collidge et al., 2010; Magee et al., 2010; Teckchandani et al., 2010; Kearney et al., 2012; Gabignon et al., 2013), and more recently, rosuvastatin (Cowan et al., 2013). The package insert for sodium fusidate (Fusidin tablets) was also recently amended with additional warnings to reflect the adverse musculoskeletal findings (https://www.medicines.org.uk/emc/medicine/2448).

The precise cause(s) of myopathy including rhabdomyolysis remains unclear. The FA package insert and the medical literature suggests inhibition of CYP3A4 by FA as a likely mechanism of muscular side effects (Burtenshaw et al., 2008; Collidge et al., 2010; Teckchandani et al., 2010; Kearney et al., 2012), since CYP3A4 is principally responsible for the metabolic clearance of atorvastatin and simvastatin in humans (Lennernäs, 2003; Elsby et al., 2012). However, it is now widely recognized that the systemic clearance of statins such as atorvastatin, simvastatin, and rosuvastatin is predominantly determined by the hepatic uptake mediated by organic anion transporting polypeptides (OATPs; OATP1B1, OATP1B3, and OATP2B1) (Neuvonen et al.,

This research was supported by Pfizer, Inc.
dx.doi.org/10.1124/dmd.115.067447.

ABBREVIATIONS: 95% CI, 95% confidence interval; AUC, area under the plasma concentration-time curve; CP-628374, (2*E*)-3-(4-{[(2*S*,3*S*,4*S*,5*R*)-5-{(1*E*)-*N*-[(3-chloro-2,6-difluorobenzyl)oxy]ethanimidoyl}-3,4-dihydroxytetrahydrofuran-2-yl]oxy}-3-hydroxyphenyl)-2-methyl-*N*-[(3*aS*,4*R*,5*R*,6*S*,7*R*,7*aR*)-4,6,7-trihydroxyhexahydro-1,3-benzodioxol-5-yl]prop-2-enamide; DDI, drug–drug interaction; ER, efflux ratio; FA, fusidic acid; F_a, fraction of the oral dose absorbed; f_u, fraction unbound; HBSS, Hanks' balanced salt solution; HEK, human embryonic kidney; HPLC, high-performance liquid chromatography; LC-MS/MS, liquid chromatography–tandem mass spectrometry; MDCKII, Madin–Darby canine kidney II; MDCKII-LE, Madin–Darby canine kidney–low efflux; MRM, multiple reaction monitoring; OATP, organic anion transporting polypeptide; P450, cytochrome P450; $t_{1/2}$, half-life; TDI, time-dependent inhibition; T_{max}, time of first occurrence of C_{max}.

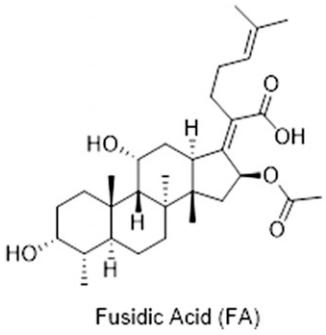

Fig. 1. Structure of FA.

2006; Kitamura et al., 2008; Zamek-Gliszczynski et al., 2009; König et al., 2013). According to the extended clearance classification system (Varma et al., 2015), statins fall into class 1B and 3B, wherein the OATP1B1-mediated hepatic uptake is the rate-determining step in their systemic clearance, although class 1B compounds (e.g., atorvastatin and simvastatin) are ultimately eliminated from the body as metabolites and class 3B statins (e.g., rosuvastatin) are eliminated unchanged in feces via biliary excretion. Several drug–drug interaction (DDI) studies indicate that OATPs inhibitors such as rifampicin and cyclosporine A exhibit a profound effect on the plasma exposure of statins (Hermann et al., 2004; Lau et al., 2007). For instance, in a microdose study, the area under the plasma concentration-time curve (AUC) of atorvastatin was shown to be markedly increased upon coadministration with a single oral rifampicin dose, but not in the presence of an intravenous dose of itraconazole, a potent CYP3A4 inhibitor, indicating that OATP-mediated uptake in the liver is the rate-determining process in the hepatic clearance of atorvastatin (Maeda et al., 2011). In addition, polymorphisms in *SLCO1B1* (encoding OATP1B1) are known to alter transporter activity, leading to significant changes in systemic exposure for some statins (Elsby et al., 2012; Birmingham et al., 2015). Furthermore, several statins, including atorvastatin and rosuvastatin, are substrates for ATP-dependent efflux transporters such as multidrug resistant protein 1 (MDR1) and breast cancer resistance protein (BCRP), which facilitate their oral absorption and biliary elimination (Chen et al., 2005; Kitamura et al., 2008; Li et al., 2011).

We therefore hypothesized that the higher incidences of statin-induced myopathy and rhabdomyolysis in patients taking comedication with FA are principally due to its inhibitory effects on hepatobiliary transporters and metabolizing enzymes responsible for statin disposition. Consequently, we evaluated the in vitro inhibitory potential of FA against major drug transporters, OATP1B1, OATP1B3, MDR1, and BCRP. Furthermore, the reversible inhibition and time-dependent inhibition (TDI) of CYP3A4 was assessed with FA using human liver microsomes. In addition, an oral DDI study between FA and rosuvastatin was conducted in rats to examine the relevance of the in vitro inhibitory effects of FA on rat Oatp1a4 and Oatp1b2 in an in vivo system.

Materials and Methods

General Chemicals. FA sodium salt (purity ≥ 98%), monobasic and dibasic potassium phosphate buffer, magnesium chloride, and NADPH were purchased from Sigma-Aldrich (St. Louis, MO). Commercially obtained chemicals and solvents were of high-performance liquid chromatography (HPLC) or analytical grade. Pooled male and female human liver microsomes (n = 50 donors) were purchased from BD Gentest (Woburn, MA). Midazolam was purchased from Cerilliant Corp. (Austin, TX), whereas 1′-hydroxymidazolam, and 1′-hydroxymidazolam-d_4 were synthesized at Pfizer Inc (Groton, CT). Rosuvastatin calcium was purchased from Sequoia Research Products (Pangbourne, UK).

CYP3A4 Inhibition Studies. Reversible inhibition of human CYP3A4 by FA was evaluated in pooled human liver microsomes (protein concentration = 0.05 mg/ml) in the presence of NADPH (1.3 mM) in 100 mM potassium phosphate buffer, pH 7.4, containing 3.3 mM $MgCl_2$ at 37°C open to air. The incubation volume was 0.2 ml and four replicates were included per FA concentration. Incubation mixtures contained FA at concentrations ranging from 0.1 to 1000 μM and midazolam (4 μM) as the probe CYP3A4 substrate. At the end of the incubation period (5 minutes), acetonitrile containing 1′-(d_4)-hydroxymidazolam (0.1 μg/ml) as internal standard was added, and the mixture was centrifuged (2000 × g, 5 minutes at room temperature). The concentration of midazolam used in the assay approximated its K_M value that had been previously determined, and the incubation time was selected based on previous determinations of reaction velocity linearity (Walsky and Obach, 2004). The supernatant was mixed with an equal volume of water containing 0.2% formic acid and was then analyzed by liquid chromatography–tandem mass spectrometry (LC-MS/MS) for 1′-hydroxymidazolam using validated bioanalytical conditions established previously (Walsky and Obach, 2004). Formation of 1′-hydroxymidazolam was quantitated using Analyst software (version 1.6; Sciex, Framingham, MA). Standard curve regression used linear regression with $1/x^2$ weighting. Resulting 1′-hydroxymidazolam concentrations were normalized to concentrations measured in solvent controls. The IC_{50} value was calculated with GraphPad software (version 6; GraphPad Software, San Diego, CA) using the log(inhibitor) versus normalized response equation assuming a Hill slope of −1.0; automatic outlier determination was enabled and no curve fitting restraints were included.

To examine the ability of FA to act as a time- and concentration-dependent inhibitor of human CYP3A4, incubations were carried out with seven FA concentrations in duplicate. Inactivation kinetic experiments have been described previously (Ghanbari et al., 2006; Obach et al., 2007; Polasek and Miners, 2007). Human liver microsomes (0.3 mg/ml), $MgCl_2$ (3.3 mM), and NADPH (1.3 mM) in potassium phosphate buffer (100 mM, pH 7.4) were prewarmed in a dry heat bath at 37°C for 5 minutes. Incubation was initiated with the addition of inhibitor or control solvent (2 μl, final incubation volume 0.2 ml). Inhibitor stock solutions were prepared in water at 100 times the final incubation concentration. Inhibitor concentrations, between 3 and 500 μM, were approximately evenly spaced after applying a log transformation. At several time points (1.0, 5.0, 10, 20, 30, and 40 minutes), an aliquot of the incubation mixture (10 μl) was transferred to a prewarmed activity incubation mixture, consisting of midazolam (23 μM, approximately 10-fold K_M), $MgCl_2$ (3.3 mM), and NADPH (1.3 mM) in potassium phosphate buffer (100 mM, pH 7.4) at a final volume of 200 μl, resulting in a 20-fold dilution. After 6 minutes, the activity incubation was terminated by transferring 100 μl incubated sample to 200 μl acetonitrile containing internal standard [1′-(d_4)-hydroxymidazolam, 0.1 μg/ml]. Samples were then vortexed and centrifuged for 5 minutes at 2000g at room temperature. Clean supernatant was mixed with an equal volume of water containing 0.2% formic acid and analyzed via LC-MS/MS.

LC-MS/MS Methodology for Quantitation of 1′-Hydroxymidazolam. A Sciex 6500 triple quadrupole mass spectrometer fitted with an electrospray ion source operated in positive ion mode was used to monitor for 1′-hydroxymidazolam and 1′-(d_4)-hydroxymidazolam. An Agilent 1290 binary pump (Agilent Technologies, Santa Clara, CA) with a CTC Leap autosampler (Leap Technology, Carrboro, NC) was programmed to inject 10 μl sample on a Halo 2.7-μm C18 2.1-mm × 30-mm column (Advanced Materials Technology, Wilmington, DE). A binary gradient was used to elute analytes and consisted of 0.1% (v/v) formic acid in water (mobile phase A) and 0.1% (v/v) formic acid in acetonitrile (mobile phase B) at a flow rate of 0.5 ml/min. Analytes were monitored using multiple reaction monitoring (MRM) mode for the mass-to-charge transitions 342.2 → 324.2 [1′-hydroxymidazolam] and 346.2 → 328.2 [1′-(d_4)-hydroxymidazolam]. Analytes were quantified versus a standard curve using Analyst. The linear range of the 1′-hydroxymidaozlam standard curve was 1–500 nM. Quality control samples contained inhibitor at the highest concentration tested in the activity incubation and indicated that FA did not suppress the 1′-hydroxymidazolam signal.

Estimation of Kinetic Constants for TDI of CYP3A4. The percent activity remaining was obtained by normalizing the concentration of 1′-hydroxymidazolam formed in each sample to the mean solvent control at the first time point. The natural log (ln) of the percentage remaining activity was plotted against the preincubation time. The slope ($-k_{obs}$) of each line was then calculated for the linear portion of the curve using GraphPad Prism software (version 6). The

automatic outlier elimination function was enabled. The details of the statistical TDI data analysis have been described by Yates et al. (2012) and were performed using Microsoft Excel (Redmond, WA). A statistical test was applied at each inhibitor concentration to evaluate whether k_{obs} was significantly different from the solvent control (eq. 1).

$$z = \frac{\left| k_{obs[I]} - k_{obs[0\mu M]} \right|}{\sqrt{S.E._{k_{obs[I]}}^2 + S.E._{k_{obs[0\mu M]}}^2}} \quad (1)$$

In this equation, $k_{obs[I]}$, $k_{obs[0\ \mu M]}$, and S.E. represent the inactivation rate at each inhibitor concentration, inactivation rate with solvent control, and standard error, respectively. When $P < 0.05$, there is statistically significant or measureable TDI. The K_I and k_{inact} were calculated from the nonlinear regression of a three-parameter Michaelis-Menten equation (eq. 2) using GraphPad Prism.

$$k_{obs} = k_{obs[0\mu M]} + \frac{k_{inact} \times [I]}{K_I + [I]} \quad (2)$$

Cocktail Assay for Examining Cytochrome P450 Inhibition. The cocktail cytochrome P450 (P450) IC_{50} protocol has been previously described (Zientek et al., 2008). In brief, incubations were conducted in triplicate at various FA concentrations (0, 0.03, 0.1, 0.3, 1, 3, 10, and 30 μM). P450 probe substrates were 2 μM tacrine (CYP1A2), 5 μM taxol (CYP2C8), 5 μM diclofenac (CYP2C9), 40 μM *S*-mephenytoin (CYP2C19), and 5 μM dextromethorphan (CYP2D6). Incubations contained human liver microsomes (0.1 mg/ml) and NADPH (1.3 mM) and incubation time was 8 minutes. After determination of peak area ratios in Analyst, data normalization and IC_{50} curve fitting were done using IDBS E-Workbook 2013 (ID Business Solutions, London, UK).

OATP Inhibition Studies. Human embryonic kidney (HEK) 293 cells stably transfected with rat Oatp1b2 and human OATP1B1 and OATP1B3 were generated at Pfizer Inc. (Sandwich, UK). Rat Oatp1a4 was expressed in HEK-tetracycline inducible cells obtained through collaboration with Xenoport, Inc. (Santa Clara, CA). HEK cells transfected with the individual transporters were grown in Dulbecco's modified Eagle's medium containing 10% heat-inactivated fetal bovine serum. Cells were seeded at a density of 1.0×10^5 (rat Oatp1a4), 5.0×10^4 (rat Oatp1b2), or 7.0×10^4 (human OATP1B1/1B3) cells per well on BioCoat 96-well poly(D-lysine)–coated plates (Corning Inc., Corning, NY). Oatp1a4-HEK293 cells were treated with 2 mM sodium butyrate and 1 μg/μl doxycycline 48 hours prior to experimentation. For inhibition assays, the uptake of 5 μM rosuvastatin was investigated in the absence and presence of FA over a concentration range of 0.095–300 μM. After a 30-minute preincubation with uptake buffer [Hanks balanced salt solution (HBSS) supplemented with 20 mM HEPES, pH 7.4] containing FA, cells were incubated for 3 minutes in triplicate at 37°C with 0.05 ml uptake buffer containing rosuvastatin with and without FA. Cellular uptake was terminated by quickly washing the cells four times with 0.2 ml ice-cold uptake buffer. The cells were then lysed with 100 μl ice-cold methanol containing indomethacin (0.1 μg/ml) as the internal standard. The lysate was mixed with 100 μl water, vigorously vortex-mixed, and a 10-μl aliquot was injected onto an LC-MS/MS system. LC-MS/MS analysis was performed on an AB Sciex Triple Quad 4000 mass spectrometer (TurboIonSpray interface) with Shimadzu LC-20AD Prominence HPLC pumps (Shimadzu Scientific Instruments, Columbia, MD) and a CTC Analytics Leap Technologies HTC PAL autosampler. The HPLC flow rate was 0.3 ml/min. A gradient method was used with samples loaded onto a Phenomenex XB-C18 30-mm × 2.1-mm column (Phenomenex, Torrence, CA) using 0.1% formic acid in water (mobile phase A) and 0.1% formic acid in acetonitrile (mobile phase B). Samples were eluted using a gradient that began with 10% B for the first 0.5 minute, which was then linearly increased to 90% B at 1.25 minutes and held at this mixture for 0.25 minute before reverting back to initial solvent conditions for 0.5 minute to re-equilibrate the column. MRM transitions used for monitoring rosuvastatin and indomethacin in negative ion mode were 480.3 → 418.2 and 356.0 → 311.8, respectively. Collision-induced dissociation spectra were acquired with Analyst (version 1.6.2), and MultiQuant (version 3.0.2; Sciex, Framingham, MA) was used for quantitation.

MDR1 and BCRP Inhibition Protocol. Madin–Darby canine kidney II (MDCKII)-MDR1 cells were acquired from Dr. Piet Borst (The Netherlands Cancer Institute, The Netherlands, Amsterdam), whereas Madin–Darby canine kidney–low efflux (MDCKII-LE)-BCRP cells (Di et al., 2011) were generated at Pfizer Inc. MDR1 and BCRP inhibition studies were conducted using previously described methodology. Briefly, MDCKII-MDR1 and MDCKII-LE-BCRP cells were grown in minimum essential medium α nucleosides (Life Technologies, Grand Island, NY) supplemented with 10% fetal bovine serum, 1% minimum nonessential amino acids solution, 1% GlutaMAX, and 1% penicillin-streptomycin prior to seeding into Millipore 96-well cell culture insert plates (EMD Millipore Corporation, Billerica, MA) for MDR1 and Corning HTS Transwell 96-well plates. The MDCKII-MDR1 and MDCKII-LE-BCRP cells were cultured on the inserts with 75 μl medium per well on the apical side and 36 ml for all 96 wells on the basolateral side. The effect of multiple concentrations of FA (0.1–500 μM) on the bidirectional permeability of digoxin (10 μM) and pitavastatin (2 μM) across MDCKII-MDR1 and MDCKII-LE-BCRP cells, respectively, was measured to determine inhibitory effects. The cell culture medium was removed, and the cells were rinsed with HBSS and preincubated for 10 minutes to allow the cells to adjust to the buffer. The donor solutions, containing digoxin or pitavastatin in HBSS at a single concentration alone and in the presence of increasing concentrations of FA, were added to the donor chambers (apical, 75–100 μl; or basolateral, 250–300 μl). HBSS or HBSS containing the matching donor concentrations of FA was added to the receiver chambers. After 90-minute incubations, aliquots (50–60 μl) were taken from the receiver chambers to determine the translocated amount of digoxin or pitavastatin. Samples were taken from the donor chambers before and after incubation to determine the initial concentration (C_0) (5–10 μl plus 190–295 μl HBSS). An internal standard solution, 120 and 180 μl 0.5 μg/ml internal standard (CP-628374 [(2*E*)-3-(4-{[(2*S*,3*S*,4*S*,5*R*)-5-{(1*E*)-*N*-[(3-chloro-2,6-difluorobenzyl)oxy]ethanimidoyl}-3,4-dihydroxytetrahydrofuran-2-yl]oxy}-3-hydroxyphenyl)-2-methyl-*N*-[(3*aS*,4*R*,5*R*,6*S*,7*R*,7*aR*)-4,6,7-trihydroxyhexahydro-1,3-benzodioxol-5-yl]prop-2-enamide], molecular weight = 687.04) in 100% methanol, was added to the receiver and donor samples, respectively. The samples were analyzed by LC-MS/MS to determine the peak area for digoxin, pitavastatin, and the internal standard. LC-MS/MS protocols for the analysis of digoxin and pitavastatin have been published (Yao et al., 2003; Hirano et al., 2005). All incubations assessing the inhibitory effect of FA on MDR1 and BCRP were conducted in triplicate.

Apparent permeability values (P_{app}) were calculated according to the following equation (eq. 3):

$$P_{app} = \frac{dx/dt}{C_0 \times A} \quad (3)$$

where dx is the amount of compound in the receiver compartment, dt is the incubation time, and A is the area of the filter of the transwell plate.

Efflux ratio (ER) values were calculated according to the following equation (eq. 4):

$$Efflux\ Ratio = \frac{P_{app,B\text{-}A}}{P_{app,A\text{-}B}} \quad (4)$$

Percent efflux values were calculated according to the following equation (eq. 5):

$$Percent\ Efflux_{MDR1} = \frac{ER_{probe+inhibitor}}{ER_{probe}} \times 100\% \quad (5)$$

From the percent ERs of probe, IC_{50} values for inhibition of efflux of probe substrates were determined with GraphPad Prism 6 using the following equation (eq. 6) as described by Rautio et al. (2006):

$$Activity = \frac{100\%}{1 + \left(I/IC_{50}\right)^s} \quad (6)$$

where I is the inhibitor concentration and s is the slope factor. The IC_{50} values for inhibition of uptake and efflux transporters were determined by fitting the percentage of inhibition-concentration data into the Hill equation.

Prediction of DDI Potential of FA Using a Static (*R*) Model. The magnitude of DDI arising via inhibition for OATP1B1-mediated hepatic uptake (R value) by FA was calculated using eq. 7 (Giacomini et al., 2013; Tweedie et al., 2013):

$$R = 1 + \frac{I_{in,max,u}}{K_i} \quad (7)$$

where K_i would represent the inhibition constant for OATP1B1 by FA and $I_{in,max,u}$ represents the estimated maximum unbound FA concentration at the inlet to the liver and is defined as follows (Ito et al., 2002).

$$I_{in,max,u} = f_{u,b} \times \left(C_{max} + \frac{k_a \times F_a \times F_g \times dose}{Q_h} \right) \quad (8)$$

$$k_a = \frac{0.693}{\text{absorption } t_{1/2}} \quad (9)$$

where, $f_{u,b}$ is the unbound fraction of FA in blood and is assumed to be equal to f_u in plasma (i.e., the blood-to-plasma ratio is assumed to be unity), C_{max} is the maximal systemic exposure after oral dosing, F_a is fraction of the oral dose absorbed from the gut to the portal vein, F_g is the fraction of the absorbed inhibitor dose escaping gut wall extraction, k_a is the oral absorption rate constant, and Q_h is the human hepatic blood flow of 97 l/h per 70 kg (Yang et al., 2007).

DDI Study Between Rosuvastatin and FA in Rats. For the rat pharmacokinetic DDI study between rosuvastatin and FA, oral doses targeted $I_{in,max,u}$ above the human OATP1B1 IC_{50} value of 1.59 μM (assumed to be equal to K_i) for FA. Oral pharmacokinetics parameters C_{max} and time of occurrence of C_{max} (i.e., T_{max}) of 1.32 μg/ml and 0.25 hour, respectively, for a 100-mg/kg oral dose of FA in rats, were obtained from the literature (http://www.cempra.com/common/pdf/Posters/From%20Mouse%20to%20Man.pdf). For setting doses, linear increases in C_{max} values from 1.32 μg/ml to 3.3 μg/ml (1.32 μg/ml $\times$ 2.5) for FA were assumed. Absorption half-life ($t_{1/2}$) was estimated as T_{max}/5, or 0.05 hours for FA. The fraction of the oral dose absorbed (F_a) was assumed as 1.0 leading to a dose of 250 mg/kg for FA. FA rat plasma f_u was 0.015 (Pfizer in-house measurement), whereas the blood-to-plasma ratio was set at unity. We anticipated the $I_{in,max,u}$ value to be 12 μg/ml (24 μM) for FA in rats. A low victim drug dose, 3 mg/kg rosuvastatin, was selected such that $I_{in,max,u}$ would be less than its OATP1B1 K_M or 9 μM (Sharma et al., 2012).

Pharmacokinetics studies were done at BioDuro, Pharmaceutical Product Development Inc. (Shanghai, PRC); animal care and in vivo procedures were conducted according to guidelines from the BioDuro Institutional Animal Care and Use Committee, respectively. Male jugular vein-cannulated Wistar-Hannover rats (246–259 g) were purchased from Vital River (Beijing, China). Animals were housed individually during the course of the pharmacokinetics experiments. Animals were fasted overnight before dosing and were fed after collection of the 4-hour blood samples, whereas access to water was provided ad libitum. Test compounds were administered orally as suspensions to rats (n = 3) in 0.5% carboxymethylcellulose (m/v) in water. Doses were 3 mg/kg rosuvastatin and 250 mg/kg FA; dose volume was 5 ml/kg for both compounds. Group 1 received control vehicle 15 minutes prior to rosuvastatin and group 2 received FA 15 minutes prior to rosuvastatin. Blood was collected into cold tubes containing K_2EDTA, stored on wet ice, and centrifuged at 2000g for 10 minutes at 4°C to obtain plasma. Plasma was mixed with an equal volume of 0.1 M sodium acetate buffer (pH 4.0) to prevent ex vivo interconversion between rosuvastatin and its lactone (Macwan et al., 2012) and was stored frozen until analysis. Blood samples were taken prior to administration of test compound or vehicle and at various time points after dosing [group 1 (−0.25 hour dose control vehicle; 0 hour dose rosuvastatin): 0, 0.083, 0.25, 0.5, 1, 2, 4, and 7 hours; and group 2 (−0.25 hour dose FA): −0.0167 hours, −0.083 hours (0 hour dose rosuvastatin), 0.083, 0.25, 0.5, 1, 2, 4, and 7 hours]. Aliquots of buffered plasma (50 μl) were transferred to 96-well plates on wet ice and then acetonitrile (200 μl) containing 0.1% acetic acid and an internal standard (25 ng/ml terfenadine) was added to each well. Samples were vortexed for 1 minute and centrifuged at 2000g for 15 minutes. Supernatant was removed and mixed with 10 volumes of water containing formic acid (0.1%). These samples were analyzed by LC-MS/MS, and concentrations of analyte in plasma were determined by interpolation from a standard curve.

A Sciex 4000 or 5500 triple quadrupole mass spectrometer fitted with an electrospray ion source operated in positive ion mode was used to monitor for analytes and internal standard. Shimadzu LC-20AD pumps with a CTC Leap autosampler were programmed to inject 3 or 8 μl sample on a Phenomenex Kinetics 2.6 μm C18 3-mm $\times$30-mm column at room temperature. A binary gradient was used to elute analytes and consisted of 0.05% (v/v) formic acid and 5 mM ammonium acetate in water (mobile phase A) and 0.1% (v/v) formic acid in acetonitrile (mobile phase B) at a flow rate of 0.5 ml/min. For rosuvastatin, the initial mobile phase composition was 25% B held for 0.4 minutes, ramped to 95% B over 0.3 minutes and held for 1 minute, and mobile phase was returned to initial conditions for 1.3 minutes. For FA, the initial mobile phase composition was 25% B held for 0.4 minutes, ramped to 95% B over 1.8 minutes and held for 0.3 minutes, and mobile phase was returned to initial conditions for 1 minute. Analytes were monitored using MRM mode for the mass-to-charge transitions 482.2 → 258.2 (rosuvastatin), 534.5 → 457.4 (FA), and 472.4 → 436.4 (terfenadine). LC-MS/MS analysis was done using Analyst software version 1.5 or 1.6. Watson LIMS 7.4 software (Thermo Scientific, Waltham, MA) was used for standard curve regression using linear regression with $1/x^2$ weighting. The linear range of each analyte was 0.5–1000 ng/ml for rosuvastatin and 10–10,000 ng/ml for FA.

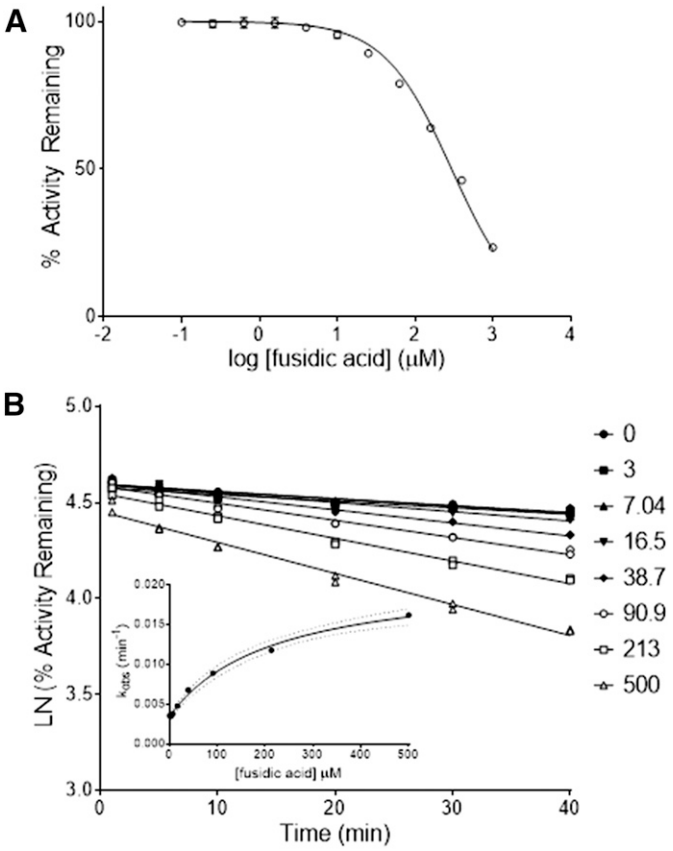

Fig. 2. Reversible (A) and time-dependent (B) inhibition of CYP3A4-catalyzed midazolam-1′-hydroxylase activity in human liver microsomes by FA. (A) Competitive inhibition plot of percent activity remaining (1′-hydroxymidazolam formation) versus log of FA concentration. Values are plotted as the mean (n = 4) and error bars indicate the S.D. Curve fitting was used to determine IC_{50}. (B) TDI, natural log (LN) of percent activity remaining (1′-hydroxymidazolam formation) versus FA concentration. Concentrations are shown in the legend. Linear regression was used to calculate the negative slope (k_{obs}) at each FA concentration. The inset shows TDI k_{obs} plotted versus FA concentrations and a three-parameter nonlinear regression was performed to calculated K_I and k_{inact}. The solid line illustrates the line of best fit and the dotted lines represent the 95% confidence band.

Determination of Pharmacokinetic Parameters. Pharmacokinetic parameters were determined with noncompartmental analysis using Watson LIMS 7.4 software. C_{max} and T_{max} values in plasma were estimated directly from the individual plasma concentration-time curves, with T_{max} defined as the time of first occurrence of C_{max}. The AUC from time 0 to the last sampling point was estimated using the linear trapezoidal rule. The terminal slope (k_{el}) of the ln (concentration) versus time plot was calculated by linear least-squares regression and the $t_{1/2}$ was calculated as 0.693 divided by the absolute value of the slope.

Statistical Analysis. An unpaired one-tailed t test was used to assess significance of differences in the DDI studies, comparing the test group with the control. In instances where parameters possessed unequal variances ($P <$ 0.05), analysis was performed with Welch's correction. In all cases, $P < 0.05$ was predetermined as the criterion for significance. All statistical analysis was performed using GraphPad Prism software (version 6).

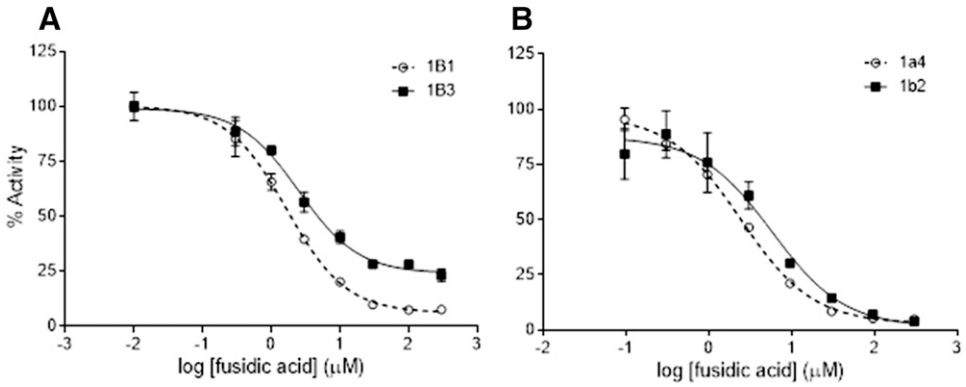

Fig. 3. Concentration-dependent inhibition of human OATP1B1 and OATP1B3 (A) and rat Oatp1a4 and Oatp1b2 (B) uptake transporters by FA. Transporter inhibition was investigated by determining the uptake of rosuvastatin (5 μM) in the HEK cell line overexpressing the respective transporters. Data are expressed as the mean of three replicates and error bars represent the S.D.

Results

Inhibition of CYP3A4 by FA. The ability of FA to inhibit CYP3A4-catalyzed midazolam-1′-hydroxylase activity was examined in human liver microsomes. Coincubation of FA (0.1–1000 μM) with midazolam (4 μM) in human liver microsomes resulted in weak reversible inhibition of CYP3A4 activity. The corresponding IC_{50} was 295 $\pm$ 1.0 μM (Fig. 2). FA also demonstrated weak time- and concentration-dependent inhibition of midazolam-1′-hydroxylase activity in human liver microsomes with estimated K_I and k_{inact} values of 216 $\pm$ 41 μM and 0.0179 $\pm$ 0.001 min^{-1}, respectively (Fig. 2). Virtually no reversible inhibition ($IC_{50} > 30$ μM) of CYP1A2, CYP2C8, CYP2C9, CYP2C19, and CYP2D6 activities in human liver microsomes was noted with FA in the cocktail IC_{50} assay.

Inhibition of Major Drug Transport Proteins by FA. Inhibitory potency of FA against major human hepatobiliary transporters, including OATP1B1, OATP1B3, MDR1, and BCRP, was tested in vitro using transporter-transfected cell lines. FA demonstrated potent inhibition of rosuvastatin uptake by OATP1B1 and OATP1B3 with IC_{50} values of 1.59 μM [95% confidence interval (95% CI), 1.48–1.78] and 2.47 μM [95% CI, 2.01–3.02], respectively (Fig. 3). On the other hand, FA demonstrated weak inhibition (IC_{50} = 157 μM; 95% CI, 105.2–234.1) of MDR1-mediated digoxin transport (Fig. 4), while showing no inhibitory effects on BCRP-mediated transport of probe substrate pitavastatin ($IC_{50} > 500$ μM). In addition, FA inhibited rosuvastatin uptake by the corresponding rat transporters rOatp1a4 and rOatp1b2, with IC_{50} values of 2.26 μM (95% CI, 2.00–2.54) and 4.38 μM (95% CI, 2.30–8.36), respectively (Fig. 3).

The magnitude of clinical DDI (calculation of R value) for inhibition of OATP1B1-mediated hepatic was estimated using a static model (eqs. 7–9) depicted in the *Materials and Methods*. The total FA C_{max} at the clinically efficacious dose (500 mg, three times daily) of FA ranges from 50 to 100 μg/ml (https://www.medicines.org.uk/emc/medicine/2448) ($C_{max,u}$ of 600–1200 ng/ml or 1.16–2.32 μM; plasma f_u value of 0.012, Pfizer data on file; molecular weight of FA = 516.7). T_{max}, reported by Still et al. (2011), was 2 hours, resulting in k_a of 1.7 h^{-1}, and F_a and F_g were set to unity. As such, the assumptions around F_a and F_g in the estimation of $I_{in,max,u}$ are reasonable considering that the pharmacokinetics of FA in humans are prototypic of carboxylic acid–based drugs with a low plasma clearance (0.3 ml/min per kilogram) and an oral bioavailability > 90% (Turnidge, 1999). The corresponding $I_{in,max,u}$ and R values were approximately 1.4–2.5 μM and 1.9–2.6, respectively, utilizing a OATP1B1 inhibition K_i value equal to its IC_{50} value of 1.59 μM, which is a reasonable assumption (Cheng and Prusoff, 1973) considering that the human OATP inhibition studies used a rosuvastatin substrate concentration approximately 4-fold below its previously estimated K_m value of 20 μM (Pfizer data on file). The K_M value for rosuvastatin uptake in HEK-OATP1B1 cells, generated in our laboratory, is in good agreement with a previously reported value of approximately 13 μM (van de Steeg et al., 2013). Suffice to say, our prediction of K_i (equal to the OATP1B1 IC_{50} value) also assumes that OATP1B1 inhibition by FA is competitive in nature. This is attributable to the fact that our OATP inhibition studies instituted a preincubation step with FA to capture any time-dependent OATP inhibitory component like the one noted with cyclosporine (Amundsen et al., 2010; Shitara et al., 2012; Gertz et al., 2013).

DDI Study in Rats. To assess potential DDI between rosuvastatin and FA, a single-dose oral DDI study was conducted with male Wistar-Han rats. The plasma concentration-time profile of rosuvastatin after administration of rosuvastatin alone or in combination with FA is presented in Fig. 5. The administration of FA (250 mg/kg), 0.25 hours (approximate T_{max}) before the dosing of rosuvastatin (3 mg/kg), resulted in a significant increase (approximately 25-fold) in rosuvastatin systemic exposure [i.e., $AUC_{(0-tlast)}$ of 15 $\pm$ 5.8 versus 369 $\pm$ 90 ng·h/ml, respectively] (Table 1). Treatment with FA also caused a substantial increase (approximately 19-fold) in the C_{max} (from 7.63 $\pm$ 3.99 to 147 $\pm$ 54.5 ng/ml). The $t_{1/2}$ of rosuvastatin was similar between the two treatments (i.e., 2.3 versus 3.5 hours). After oral administration at 250 mg/kg (see Fig. 5, inset), systemic exposure of FA as assessed from $AUC_{(0-tlast)}$ was 15,167 ng·h/ml. The corresponding C_{max} was 5233 ng/ml and occurred at a T_{max} of 1.6 hours (k_a = 0.036 min^{-1}), which is

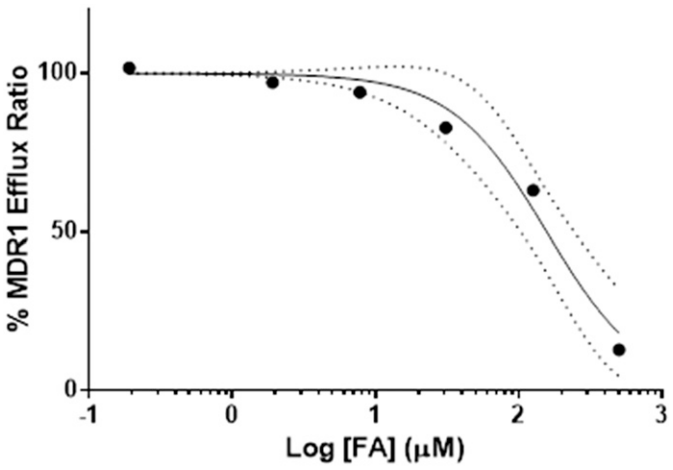

Fig. 4. Concentration-dependent inhibition of human MDR1 by FA. Inhibition of MDR1 activity was investigated by determining the digoxin efflux across MDR1-MDCKII monolayers. Data are expressed as the mean of three replicates. The solid line illustrates the line of best fit and the dotted lines represent the 95% confidence band.

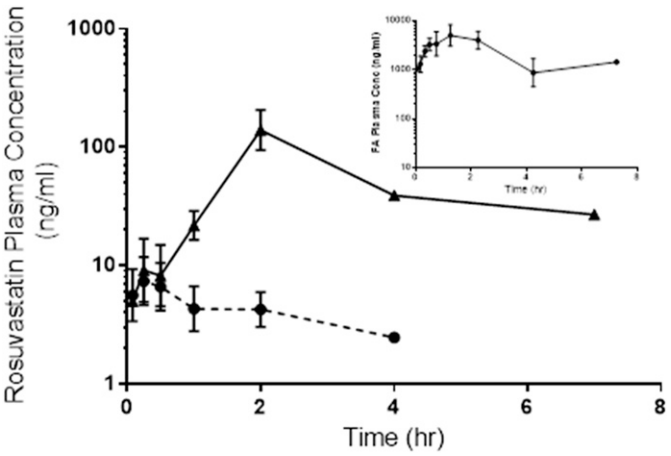

Fig. 5. Mean plasma concentration-time profile of rosuvastatin in male Wistar-Han rats after a single oral dose of rosuvastatin (3 mg/kg) and after a single oral dose of rosuvastatin (3 mg/kg) dosed 0.25 hours after oral FA (250 mg/kg). Data are expressed as means ± S.D. (n = 3 animals). Control rosuvastatin animals are represented with circles and FA with filled triangles. The inset shows the mean plasma concentration-time profile of FA in male Wistar-Han rats (n = 3) after a single oral dose of 250 mg/kg.

longer than the previously reported value of 0.25 hours (http://www.cempra.com/common/pdf/Posters/From%20Mouse%20to%20Man.pdf).

Discussion

Contrary to speculations in the product label, FA was a weak reversible and weak time-dependent inhibitor of CYP3A4 activity in human liver microsomes. Although systematic clinical DDI studies between FA and drugs metabolized by CYP3A4 have not been performed, our data suggest that muscular toxicity of statins is unlikely to be mediated via inhibitory effects of FA on hepatic CYP3A4 activity, especially in light of the relatively low unbound maximal systemic concentrations (1.16–2.32 μM) at its efficacious dosing regimen. Rather, this work demonstrates that musculoskeletal toxicity may arise through FA's inhibitory effects on OATP in the liver, which could inhibit hepatic uptake and lead to excessive blood and tissue levels of statins in the clinic in a manner similar to that noted with other OATP inhibitors (Moßhammer et al., 2014). This hypothesis is attractive because it collectively accounts for the rhabdomyolysis noted with all statins, including rosuvastatin, which is not metabolized by CYP3A4 (Martin et al., 2003), and as such, is not prone to DDIs via P450 inhibition (Neuvonen, 2010).

The inhibitory effects of FA against OATPs are consistent with a previous report by De Bruyn et al., (2013), wherein a high-throughput OATP1B1 and OATP1B3 inhibition assay monitoring for sodium fluorescein uptake noted inhibition by FA (OATP1B1 and OATP1B3 inhibition of 39.5% and 58.3% at a single FA concentration of 10 μM). In hindsight, the inhibitory effects of FA against OATP isoforms with potency comparable to established inhibitors (Izumi et al., 2015) are not altogether surprising. FA contains a lipophilic [molecular weight = 516.7, calculated topological surface area = 104 Å^2, calculated LogP = 7.28, $\text{LogD}_{(\text{pH } 7.4)}$ = 2.66] steroidal nucleus with a carboxylic acid (pK_a = 5.7) group (Turnidge, 1999). These structural and physicochemical attributes are in accordance with known structure-activity relationships for OATP interaction properties of small molecule xenobiotics including drugs (Karlgren et al., 2012a,b; Varma et al., 2012). Furthermore, because FA shares structural features with adrenocorticoids and bile salts (e.g., cholate and taurocholate), it is possible that Na^+-taurocholate cotransporting polypeptide (expressed at the sinusoidal membrane of hepatocytes), which is also involved in statin uptake (Bi et al., 2013; Vildhede et al., 2014), is prone to inhibition by FA.

The assessment of OATP1B-mediated DDIs with certain chemotypes (e.g., anionic small molecule drug candidates) has become a critical aspect of early drug development as recognized in draft guidance issued by the regulatory agencies in the United States (U.S. Food and Drug Administration Center for Drug Evaluation and Research, 2012; http://www.fda.gov/downloads/drugs/guidancecomplianceregulatoryinformation/guidances/ucm292362.pdf), the European Union (Committee for Human Medicinal Products, 2012; http://www.ema.europa.eu/docs/en_GB/document_library/Scientific_guideline/2012/07/WC500129606.pdf) and the International Transporter Consortium (Giacomini et al., 2013; Tweedie et al., 2013). These guidance documents/perspectives acknowledge OATP1B1 and OATP1B3 as two of the seven clinically relevant transporters and provide basic methodology toward the prediction of the DDI magnitude with OATP inhibitors. One such methodology utilizes the static (R) model: $R = (1 + I_{in,max,u}/K_i)$, wherein the likelihood of DDI due to OATP inhibition would increase with an R value > 1.25. The magnitude of DDI resulting from inhibition of OATP1B1-mediated hepatic uptake by FA was approximated to be 1.9–2.6, suggesting that FA could potentially cause clinical DDI with drugs (e.g., statins) that are prone to hepatic uptake by OATPs.

Efflux transporters MDR1 and BCRP are expressed at the canalicular membrane and are involved in the biliary efflux of statins (Li et al., 2011). These transporters are also expressed on the apical membrane of the enterocytes and are known to limit the intestinal absorption of several statins (Shitara et al., 2013). Inhibition of intestinal and/or biliary efflux (in addition to OATP inhibition) by cyclosporine A has been speculated as a potential factor for clinical DDIs with rosuvastatin, which is not susceptible to P450 metabolism (Jamei et al., 2014). In our studies, virtually no inhibitory effect ($IC_{50} > 500$ μM) of FA was discerned on BCRP-mediated transport of pitavastatin, whereas modest inhibition of digoxin transport by MDR1 (IC_{50} = 157 μM) was noted with FA. Taking into account the low unbound systemic FA concentrations, the weak MDR1 inhibition discerned in vitro is unlikely to translate into meaningful DDIs via inhibition of statin biliary efflux by MDR1. However, DDIs arising from inhibition of intestinal MDR1 by FA cannot be ruled out. For orally administered drugs, the International Transporter Consortium guidance (Tweedie et al., 2013) recommends the use of the $[I]_2$/MDR1 IC_{50} criterion to predict the DDI via intestinal MDR1 inhibition, where $[I]_2$ represents intestinal inhibitor concentration expressed as total daily dose (in moles)/250 ml (Fenner et al., 2009). Applying this criterion to FA (total daily dose = 1500 mg, molecular weight = 516.7, MDR1 IC_{50} = 157 μM) yields an $[I]_2$/MDR1 IC_{50} ratio of approximately 74, which exceeds the "cutoff" value of 10. Overall, this suggests that inhibition of MDR1 at the intestine could have contributed to the observed interaction for substrate drugs such as atorvastatin (Chen et al., 2005).

TABLE 1

Pharmacokinetic parameters of rosuvastatin after a single oral dose of 3 mg/kg to male Wistar-Han rats in the presence of vehicle or a single oral dose of FA (250 mg/kg)

Rosuvastatin was administered 0.25 hours after pretreatment with FA. Data are presented as means ± S.D. from three male rats and were derived from noncompartmental analysis.

Treatment	C_{max}	T_{max}	$t_{1/2}$	$AUC_{(0-tlast)}$
	ng/ml	*h*	*h*	*ng·h/ml*
Vehicle	7.63 ± 3.99	1.08 ± 1.01	2.29 ± 1.63	15.0 ± 5.80
FA (250 mg/kg)	147 ± 54.5[a]	2.92 ± 1.15	3.52 ± 4.25	369 ± 90.0[a]

[a] t test with Welch's correction of unpaired t test data (variances/S.D. were not equal between groups, $P < 0.05$).

To date, there are no reports of clinical DDI studies on FA. Therefore, we decided to examine the likelihood of a DDI upon oral administration of rosuvastatin (3 mg/kg) in the absence or presence of FA using rats as an in vivo model. As a prelude to the in vivo DDI studies, the inhibitory effects of FA on rosuvastatin uptake by rat Oatp isoforms were initially examined. Previous studies have shown that rosuvastatin is a substrate of rOatp1a1, rOatp1a4, and rOatp1b2, respectively, in vitro (Ho et al., 2005, 2006). Although there is no direct evidence on the percentage contribution of each isoform to the active hepatic uptake of rosuvastatin in vivo in rats, our internal transcriptomic BodyMap studies of rat liver have shown that the expression of Oatp1a4 and Oatp1b2 isoforms is significantly greater than Oatp1a1 (Pfizer data on file), which is also consistent with previous studies on mRNA expression of Oatp transporters in mice (Klaassen and Aleksunes, 2010). Consequently, we focused our attention on assessing inhibition of rat Oatp1a4- and Oatp1b2-mediated rosuvastatin transport by FA. Our in vitro studies demonstrated that FA inhibited rosuvastatin uptake mediated by rOatp1a4 and rOatp1b2 with IC_{50} values of 2.26 μM and 4.38 μM, respectively. Coadministration with FA (250 mg/kg) also led to an approximately 19.2-fold and 24.6-fold increase in rosuvastatin C_{max} and $AUC_{(0–tlast)}$, respectively. The $I_{in,max,u}$ value of approximately 3.9 μM estimated for FA was lower than the anticipated value of 24 μM due to a longer T_{max} of 1.6 hours (instead of the reported value of 0.25 hours). Nevertheless, the $I_{in,max,u}$ value is within the range of Oatp1a2/1b4 IC_{50} values; since Oatp-mediated hepatic uptake is the rate-limiting step in rosuvastatin clearance in rats (as is the case in humans), it is tempting to speculate that the origins of the DDI between rosuvastatin and FA are at least partially mediated through inhibition of rosuvastatin uptake by FA. In rats, Oatp-mediated uptake clearance of rosuvastatin is limited by hepatic blood flow (He et al., 2014), and thus a large AUC ratio (the observed AUC ratio in this study is approximately 25) is expected upon complete inhibition of transporter-mediated uptake. In humans, the hepatic extraction of rosuvastatin is approximately 60% of hepatic blood flow (Martin et al., 2003), suggesting that the magnitude of rosuvastatin–FA interaction in humans could be relatively smaller than that observed in our in vivo rat DDI study.

Against this backdrop, the synergistic contribution of FA metabolites toward inhibition of hepatobiliary transporters in humans and rodents cannot be excluded. Examination of the excretion routes in humans reveals minimal biliary, fecal, and renal excretion of unchanged FA (Godtfredsen and Vangedal, 1966; Reeves, 1987; Singlas et al., 1988), suggesting that metabolism is the principal elimination mechanism of FA in humans. Preliminary metabolite identification studies (Godtfredsen and Vangedal, 1966) using human bile revealed the presence of acyl glucuronide and dicarboxylic acid (derived from oxidation of one of the terminal methyl group) metabolites, which accounted for approximately 15% and 10% of the administered oral dose of FA, respectively. Contribution of these FA metabolites to the in vivo inhibition of hepatobiliary transport with similar or greater potency could potentially exacerbate the magnitude of DDI in the clinic and in the rat model used to probe the DDI potential of FA.

FA, although widely used throughout the world for decades, has never been approved in the United States. Given the need for a safe oral methicillin-resistant *Staphylococcus aureus* antibiotic, there has been a growing interest in pursuing FA for systemic treatment of serious infections in the United States. Oral FA has recently been studied in comparison with linezolid in a phase II clinical trial for the treatment of acute bacterial skin infections, with comparable clinical success (Craft et al., 2011). Phase II clinical studies evaluating the potential of oral FA in the treatment of prosthetic joint infections (http://www.cempra.com/products/taksta-cem-102/) are also in progress in the United States (Fernandes and Pereira, 2011). Considering the current usage and the imminent availability of FA in the United States, our studies provide a strong basis for the need to conduct relevant DDI studies with FA in the clinic.

Finally, our findings also raise an intriguing possibility that the clinical cases of hyperbilirubinemia/jaundice noted with FA use (Humble et al., 1980; Kutty et al., 1987; Haddad et al., 1993) could be potentially linked to its inhibitory effects on the OATP1B1- and OATP1B3-mediated bilirubin transport into the liver. Hepatic uptake of bilirubin by OATPs constitutes the first step in the multifaceted elimination process of the heme breakdown product (Cui et al., 2001); a combination of inhibitory effects on bilirubin uptake and/or bilirubin glucuronidation in the liver has emerged as a common theme among drugs associated with clinical hyperbilirubinemia (Chiou et al., 2014).

Acknowledgments

The authors thank Honglei Zhao and Brian Holder for technical assistance.

Authorship Contributions

Participated in research design: Eng, Scialis, Lin, Varma, Di, Feng, Kalgutkar.

Conducted experiments: Eng, Scialis, Rotter, Lazzaro, West.

Performed data analysis: Eng, Scialis, Rotter, Lin, Lazzaro, Varma, Di, Feng, Kalgutkar.

Wrote or contributed to the writing of the manuscript: Eng, Scialis, Rotter, Lin, Lazzaro, Varma, Di, Feng, Kalgutkar.

References

Aboltins CA, Page MA, Buising KL, Jenney AW, Daffy JR, Choong PF, and Stanley PA (2007) Treatment of staphylococcal prosthetic joint infections with debridement, prosthesis retention and oral rifampicin and fusidic acid. *Clin Microbiol Infect* **13**:586–591.

Amundsen R, Christensen H, Zabihyan B, and Asberg A (2010) Cyclosporine A, but not tacrolimus, shows relevant inhibition of organic anion-transporting protein 1B1-mediated transport of atorvastatin. *Drug Metab Dispos* **38**:1499–1504.

Bi YA, Qiu X, Rotter CJ, Kimoto E, Piotrowski M, Varma MV, Ei-Kattan AF, and Lai Y (2013) Quantitative assessment of the contribution of sodium-dependent taurocholate co-transporting polypeptide (NTCP) to the hepatic uptake of rosuvastatin, pitavastatin and fluvastatin. *Biopharm Drug Dispos* **34**:452–461.

Birmingham BK, Bujac SR, Elsby R, Azumaya CT, Wei C, Chen Y, Mosqueda-Garcia R, and Ambrose HJ (2015) Impact of ABCG2 and SLCO1B1 polymorphisms on pharmacokinetics of rosuvastatin, atorvastatin and simvastatin acid in Caucasian and Asian subjects: a class effect? *Eur J Clin Pharmacol* **71**:341–355.

Burtenshaw AJ, Sellors G, and Downing R (2008) Presumed interaction of fusidic acid with simvastatin. *Anaesthesia* **63**:656–658.

Chen C, Mireles RJ, Campbell SD, Lin J, Mills JB, Xu JJ, and Smolarek TA (2005) Differential interaction of 3-hydroxy-3-methylglutaryl-coa reductase inhibitors with ABCB1, ABCC2, and OATP1B1. *Drug Metab Dispos* **33**:537–546.

Cheng Y and Prusoff WH (1973) Relationship between the inhibition constant (K1) and the concentration of inhibitor which causes 50 per cent inhibition (I50) of an enzymatic reaction. *Biochem Pharmacol* **22**:3099–3108.

Chiou WJ, de Morais SM, Kikuchi R, Voorman RL, Li X, and Bow DAJ (2014) In vitro OATP1B1 and OATP1B3 inhibition is associated with observations of benign clinical unconjugated hyperbilirubinemia. *Xenobiotica* **44**:276–282.

Collidge TA, Razvi S, Nolan C, Whittle M, Stirling C, Russell AJ, Mann AC, and Deighan CJ (2010) Severe statin-induced rhabdomyolysis mimicking Guillain-Barré syndrome in four patients with diabetes mellitus treated with fusidic acid. *Diabet Med* **27**:696–700.

Cowan R, Johnson PD, Urbancic K, and Grayson ML (2013) A timely reminder about the concomitant use of fusidic acid with statins. *Clin Infect Dis* **57**:329–330.

Craft JC, Moriarty SR, Clark K, Scott D, Degenhardt TP, Still JG, Corey GR, Das A, and Fernandes P (2011) A randomized, double-blind phase 2 study comparing the efficacy and safety of an oral fusidic acid loading-dose regimen to oral linezolid for the treatment of acute bacterial skin and skin structure infections. *Clin Infect Dis* **52** (Suppl 7):S520–S526.

Cui Y, König J, Leier I, Buchholz U, and Keppler D (2001) Hepatic uptake of bilirubin and its conjugates by the human organic anion transporter SLC21A6. *J Biol Chem* **276**:9626–9630.

De Bruyn T, van Westen GJ, Ijzerman AP, Stieger B, de Witte P, Augustijns PF, and Annaert PP (2013) Structure-based identification of OATP1B1/3 inhibitors. *Mol Pharmacol* **83**:1257–1267.

Di L, Whitney-Pickett C, Umland JP, Zhang H, Zhang X, Gebhard DF, Lai Y, Federico JJ, 3rd, Davidson RE, and Smith R, et al. (2011) Development of a new permeability assay using low-efflux MDCKII cells. *J Pharm Sci* **100**:4974–4985.

Elsby R, Hilgendorf C, and Fenner K (2012) Understanding the critical disposition pathways of statins to assess drug-drug interaction risk during drug development: it's not just about OATP1B1. *Clin Pharmacol Ther* **92**:584–598.

Fenner KS, Troutman MD, Kempshall S, Cook JA, Ware JA, Smith DA, and Lee CA (2009) Drug-drug interactions mediated through P-glycoprotein: clinical relevance and in vitro-in vivo correlation using digoxin as a probe drug. *Clin Pharmacol Ther* **85**:173–181.

Fernandes P and Pereira D (2011) Efforts to support the development of fusidic acid in the United States. *Clin Infect Dis* **52** (Suppl 7):S542–S546.

Gabignon C, Zeller V, Le Guyader N, Desplaces N, Lidove O, and Ziza JM (2013) [Rhabdomyolysis following the coprescription of atorvastatin and fusidic acid]. *Rev Med Interne* **34**:39–41.

Gertz M, Cartwright CM, Hobbs MJ, Kenworthy KE, Rowland M, Houston JB, and Galetin A (2013) Cyclosporine inhibition of hepatic and intestinal CYP3A4, uptake and efflux transporters: application of PBPK modeling in the assessment of drug-drug interaction potential. *Pharm Res* **30**:761–780.

Ghanbari F, Rowland-Yeo K, Bloomer JC, Clarke SE, Lennard MS, Tucker GT, and Rostami-Hodjegan A (2006) A critical evaluation of the experimental design of studies of mechanism based enzyme inhibition, with implications for in vitro-in vivo extrapolation. *Curr Drug Metab* **7**:315–334.

Giacomini KM, Balimane PV, Cho SK, Eadon M, Edeki T, Hillgren KM, Huang SM, Sugiyama Y, Weitz D, and Wen Y, et al.; International Transporter Consortium (2013) International Transporter Consortium commentary on clinically important transporter polymorphisms. *Clin Pharmacol Ther* **94**:23–26.

Godtfredsen WO and Vangedal S (1966) On the metabolism of fusidic acid in man. *Acta Chem Scand* **20**:1599–1607.

Haddad M, Shabat S, Koren A, Stelman E, and Zelikovski A (1993) Fusidic acid induced jaundice. *Eur J Clin Microbiol Infect Dis* **12**:725–726.

Hall H, Gadhok R, Alshafi K, Bilton D, and Simmonds NJ (2015) Eradication of respiratory tract MRSA at a large adult cystic fibrosis centre. *Respir Med* **109**:357–363.

He J, Yu Y, Prasad B, Link J, Miyaoka RS, Chen X, and Unadkat JD (2014) PET imaging of Oatp-mediated hepatobiliary transport of [(11)C] rosuvastatin in the rat. *Mol Pharm* **11**: 2745–2754.

Hermann M, Asberg A, Christensen H, Holdaas H, Hartmann A, and Reubsaet JL (2004) Substantially elevated levels of atorvastatin and metabolites in cyclosporine-treated renal transplant recipients. *Clin Pharmacol Ther* **76**:388–391.

Herring R, Caldwell G, and Wade S (2009) Rhabdomyolysis caused by an interaction of simvastatin and fusidic acid. *BMJ Case Rep* **2009**:bcr03.2009.1722.

Hirano M, Maeda K, Matsushima S, Nozaki Y, Kusuhara H, and Sugiyama Y (2005) Involvement of BCRP (ABCG2) in the biliary excretion of pitavastatin. *Mol Pharmacol* **68**:800–807.

Ho RH, Tirona RG, Leake BF, Glaeser H, Lee W, Lemke CJ, Wang Y, and Kim RB (2006) Drug and bile acid transporters in rosuvastatin hepatic uptake: function, expression, and pharmacogenetics. *Gastroenterology* **130**:1793–1806.

Ho RH, Wang Y, Leake BF, and Kim RB (2005) Multiple OATP transporters mediate the cellular uptake of rosuvastatin. *Clin Pharmacol Ther* **77**:P64.

Humble MW, Eykyn S, and Phillips I (1980) Staphylococcal bacteraemia, fusidic acid, and jaundice. *BMJ* **280**:1495–1498.

Ito K, Chiba K, Horikawa M, Ishigami M, Mizuno N, Aoki J, Gotoh Y, Iwatsubo T, Kanamitsu S, and Kato M, et al. (2002) Which concentration of the inhibitor should be used to predict in vivo drug interactions from in vitro data? *AAPS PharmSci* **4**:E25.

Izumi S, Nozaki Y, Maeda K, Komori T, Takenaka O, Kusuhara H, and Sugiyama Y (2015) Investigation of the impact of substrate selection on in vitro organic anion transporting polypeptide 1B1 inhibition profiles for the prediction of drug-drug interactions. *Drug Metab Dispos* **43**:235–247.

Jamei M, Bajot F, Neuhoff S, Barter Z, Yang J, Rostami-Hodjegan A, and Rowland-Yeo K (2014) A mechanistic framework for in vitro-in vivo extrapolation of liver membrane transporters: prediction of drug-drug interaction between rosuvastatin and cyclosporine. *Clin Pharmacokinet* **53**:73–87.

Karlgren M, Ahlin G, Bergström CA, Svensson R, Palm J, and Artursson P (2012a) In vitro and in silico strategies to identify OATP1B1 inhibitors and predict clinical drug-drug interactions. *Pharm Res* **29**:411–426.

Karlgren M, Vildhede A, Norinder U, Wisniewski JR, Kimoto E, Lai Y, Haglund U, and Artursson P (2012b) Classification of inhibitors of hepatic organic anion transporting polypeptides (OATPs): influence of protein expression on drug-drug interactions. *J Med Chem* **55**:4740–4763.

Kearney S, Carr AS, McConville J, and McCarron MO; Northern Ireland Neurology Network (2012) Rhabdomyolysis after co-prescription of statin and fusidic acid. *BMJ* **345**:e6562.

Kitamura S, Maeda K, Wang Y, and Sugiyama Y (2008) Involvement of multiple transporters in the hepatobiliary transport of rosuvastatin. *Drug Metab Dispos* **36**:2014–2023.

Klaassen CD and Aleksunes LM (2010) Xenobiotic, bile acid, and cholesterol transporters: function and regulation. *Pharmacol Rev* **62**:1–96.

König J, Müller F, and Fromm MF (2013) Transporters and drug-drug interactions: important determinants of drug disposition and effects. *Pharmacol Rev* **65**:944–966.

Kutty KP, Nath IV, Kothandaraman KR, Barrowman JA, Perkins PG, Ra MU, and Huang SN (1987) Fusidic acid-induced hyperbilirubinemia. *Dig Dis Sci* **32**:933–938.

Lau YY, Huang Y, Frassetto L, and Benet LZ (2007) effect of OATP1B transporter inhibition on the pharmacokinetics of atorvastatin in healthy volunteers. *Clin Pharmacol Ther* **81**:194–204.

Lennernäs H (2003) Clinical pharmacokinetics of atorvastatin. *Clin Pharmacokinet* **42**: 1141–1160.

Li J, Volpe DA, Wang Y, Zhang W, Bode C, Owen A, and Hidalgo IJ (2011) Use of transporter knockdown Caco-2 cells to investigate the in vitro efflux of statin drugs. *Drug Metab Dispos* **39**:1196–1202.

Macwan JS, Ionita IA, and Akhlaghi F (2012) A simple assay for the simultaneous determination of rosuvastatin acid, rosuvastatin-5S-lactone, and N-desmethyl rosuvastatin in human plasma using liquid chromatography-tandem mass spectrometry (LC-MS/MS). *Anal Bioanal Chem* **402**:1217–1227.

Maeda K, Ikeda Y, Fujita T, Yoshida K, Azuma Y, Haruyama Y, Yamane N, Kumagai Y, and Sugiyama Y (2011) Identification of the rate-determining process in the hepatic clearance of atorvastatin in a clinical cassette microdosing study. *Clin Pharmacol Ther* **90**:575–581.

Magee CN, Medani SA, Leavey SF, Conlon PJ, and Clarkson MR (2010) Severe rhabdomyolysis as a consequence of the interaction of fusidic acid and atorvastatin. *Am J Kidney Dis* **56**:e11–e15.

Martin PD, Warwick MJ, Dane AL, Hill SJ, Giles PB, Phillips PJ, and Lenz E (2003) Metabolism, excretion, and pharmacokinetics of rosuvastatin in healthy adult male volunteers. *Clin Ther* **25**:2822–2835.

Moßhammer D, Schaeffeler E, Schwab M, and Mörike K (2014) Mechanisms and assessment of statin-related muscular adverse effects. *Br J Clin Pharmacol* **78**:454–466.

Neuvonen PJ (2010) Drug interactions with HMG-CoA reductase inhibitors (statins): the importance of CYP enzymes, transporters and pharmacogenetics. *Curr Opin Investig Drugs* **11**:323–332.

Neuvonen PJ, Niemi M, and Backman JT (2006) Drug interactions with lipid-lowering drugs: mechanisms and clinical relevance. *Clin Pharmacol Ther* **80**:565–581.

Obach RS, Walsky RL, and Venkatakrishnan K (2007) Mechanism-based inactivation of human cytochrome p450 enzymes and the prediction of drug-drug interactions. *Drug Metab Dispos* **35**:246–255.

O'Mahony C, Campbell VL, Al-Khayatt MS, and Brull DJ (2008) Rhabdomyolysis with atorvastatin and fusidic acid. *Postgrad Med J* **84**:325–327.

Polasek TM and Miners JO (2007) In vitro approaches to investigate mechanism-based inactivation of CYP enzymes. *Expert Opin Drug Metab Toxicol* **3**:321–329.

Rautio J, Humphreys JE, Webster LO, Balakrishnan A, Keogh JP, Kunta JR, Serabjit-Singh CJ, and Polli JW (2006) In vitro p-glycoprotein inhibition assays for assessment of clinical drug interaction potential of new drug candidates: a recommendation for probe substrates. *Drug Metab Dispos* **34**:786–792.

Reeves DS (1987) The pharmacokinetics of fusidic acid. *J Antimicrob Chemother* **20**:467–476.

Saeed NT and Azam M (2009) Rhabdomyolysis secondary to interaction between atorvastatin and fusidic acid. *BMJ Case Rep* **2009**:bcr06.2009.2040.

Sharma P, Butters CJ, Smith V, Elsby R, and Surry D (2012) Prediction of the in vivo OATP1B1-mediated drug-drug interaction potential of an investigational drug against a range of statins. *Eur J Pharm Sci* **47**:244–255.

Shitara Y, Maeda K, Ikejiri K, Yoshida K, Horie T, and Sugiyama Y (2013) Clinical significance of organic anion transporting polypeptides (OATPs) in drug disposition: their roles in hepatic clearance and intestinal absorption. *Biopharm Drug Dispos* **34**:45–78.

Shitara Y, Takeuchi K, Nagamatsu Y, Wada S, Sugiyama Y, and Horie T (2012) Long-lasting inhibitory effects of cyclosporin A, but not tacrolimus, on OATP1B1- and OATP1B3-mediated uptake. *Drug Metab Pharmacokinet* **27**:368–378.

Singlas E, Kitzis MD, Guibert J, Taburet AM, and Acar JF (1988) Pharmacokinetics of sodium fusidate in man after single and repeated infusions. *J Pharmacie Clinique* **7** (Suppl II):3341.

Still JG, Clark K, Degenhardt TP, Scott D, Fernandes P, and Gutierrez MJ (2011) Pharmacokinetics and safety of single, multiple, and loading doses of fusidic acid in healthy subjects. *Clin Infect Dis* **52** (Suppl 7):S504–S512.

Teckchandani S, Robertson S, Almond A, Donaldson K, and Isles C (2010) Rhabdomyolysis following co-prescription of fusidic acid and atorvastatin. *J R Coll Physicians Edinb* **40**:33–36.

Turnidge J (1999) Fusidic acid pharmacology, pharmacokinetics and pharmacodynamics. *Int J Antimicrob Agents* **12** (Suppl 2):S23–S34.

Tweedie D, Polli JW, Berglund EG, Huang SM, Zhang L, Poirier A, Chu X, and Feng B; International Transporter Consortium (2013) Transporter studies in drug development: experience to date and follow-up on decision trees from the International Transporter Consortium. *Clin Pharmacol Ther* **94**:113–125.

van de Steeg E, Greupink R, Schreurs M, Nooijen IH, Verhoeckx KC, Hanemaaijer R, Ripken D, Monshouwer M, Vlaming ML, and DeGroot J, et al. (2013) Drug-drug interactions between rosuvastatin and oral antidiabetic drugs occurring at the level of OATP1B1. *Drug Metab Dispos* **41**:592–601.

Vanderhelst E, De Wachter E, Willekens J, Piérard D, Vincken W, and Malfroot A (2013) Eradication of chronic methicillin-resistant Staphylococcus aureus infection in cystic fibrosis patients. An observational prospective cohort study of 11 patients. *J Cyst Fibros* **12**:662–666.

Varma MV, Chang G, Lai Y, Feng B, El-Kattan AF, Litchfield J, and Goosen TC (2012) Physicochemical property space of hepatobiliary transport and computational models for predicting rat biliary excretion. *Drug Metab Dispos* **40**:1527–1537.

Varma MV, Steyn SJ, Allerton C, and El-Kattan AF (2015) Predicting clearance mechanism in drug discovery: extended clearance classification system (ECCS). *Pharm Res* **32**:3785–3802.

Vildhede A, Karlgren M, Svedberg EK, Wisniewski JR, Lai Y, Norén A, and Artursson P (2014) Hepatic uptake of atorvastatin: influence of variability in transporter expression on uptake clearance and drug-drug interactions. *Drug Metab Dispos* **42**:1210–1218.

Walsky RL and Obach RS (2004) Validated assays for human cytochrome P450 activities. *Drug Metab Dispos* **32**:647–660.

Wang JL, Tang HJ, Hsieh PH, Chiu FY, Chen YH, Chang MC, Huang CT, Liu CP, Lau YJ, and Hwang KP, et al. (2012) Fusidic acid for the treatment of bone and joint infections caused by meticillin-resistant Staphylococcus aureus. *Int J Antimicrob Agents* **40**:103–107.

Wenisch C, Krause R, Fladerer P, El Menjawi I, and Pohanka E (2000) Acute rhabdomyolysis after atorvastatin and fusidic acid therapy. *Am J Med* **109**:78.

Yang J, Jamei M, Yeo KR, Tucker GT, and Rostami-Hodjegan A (2007) Prediction of intestinal first-pass drug metabolism. *Curr Drug Metab* **8**:676–684.

Yao M, Zhang H, Chong S, Zhu M, and Morrison RA (2003) A rapid and sensitive LC/MS/MS assay for quantitative determination of digoxin in rat plasma. *J Pharm Biomed Anal* **32**:1189–1197.

Yates P, Eng H, Di L, and Obach RS (2012) Statistical methods for analysis of time-dependent inhibition of cytochrome p450 enzymes. *Drug Metab Dispos* **40**:2289–2296.

Yuen SL and McGarity B (2003) Rhabdomyolysis secondary to interaction of fusidic acid and simvastatin. *Med J Aust* **179**:172.

Zamek-Gliszczynski MJ, Kalvass JC, Pollack GM, and Brouwer KL (2009) Relationship between drug/metabolite exposure and impairment of excretory transport function. *Drug Metab Dispos* **37**:386–390.

Zientek M, Miller H, Smith D, Dunklee MB, Heinle L, Thurston A, Lee C, Hyland R, Fahmi O, and Burdette D (2008) Development of an in vitro drug-drug interaction assay to simultaneously monitor five cytochrome P450 isoforms and performance assessment using drug library compounds. *J Pharmacol Toxicol Methods* **58**:206–214.

Address correspondence to: Amit S. Kalgutkar, Pharmacokinetics, Dynamics, and Metabolism–New Chemical Entities, Pfizer Worldwide Research and Development, 610 Main Street, Cambridge, MA 02139. E-mail: amit.kalgutkar@pfizer.com